

Supporting Information for:

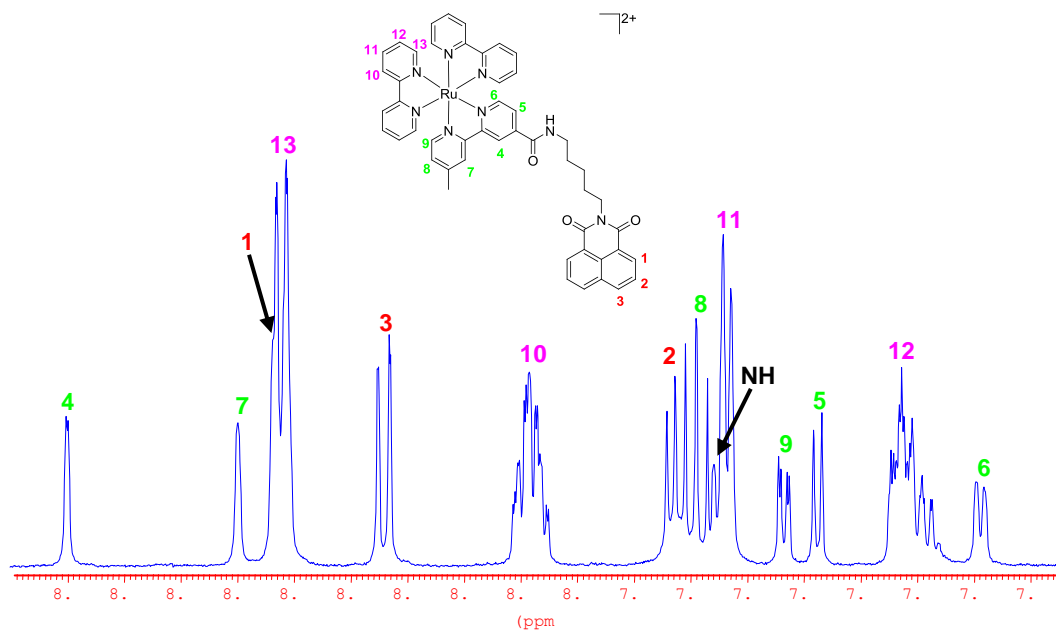
Unexpected DNA binding properties with correlated downstream biological applications in mono vs. bis-1,8-naphthalimide Ru(II)-polypyridyl conjugates

Gary J. Ryan,^a Robert B. P. Elmes,^a Marialuisa Erby,^c Fergus E. Poynton,^a D. Clive Williams,^{c*} Susan J. Quinn^{b*} and Thorfinnur Gunnlaugsson^{a*}

- a. School of Chemistry and Trinity Biomedical Science Institute, Trinity College, Dublin 2, Ireland.
- b. School of Chemistry and Chemical Biology, University College Dublin, Dublin 4, Ireland
- c. School of Biochemistry and Immunology, and Trinity Biomedical Science Institute, Trinity College, Dublin 2, Ireland

E-mail: susan.quinn@ucd.ie, gunnlaut@tcd.ie, clive.williams@tcd.ie

A)



B)

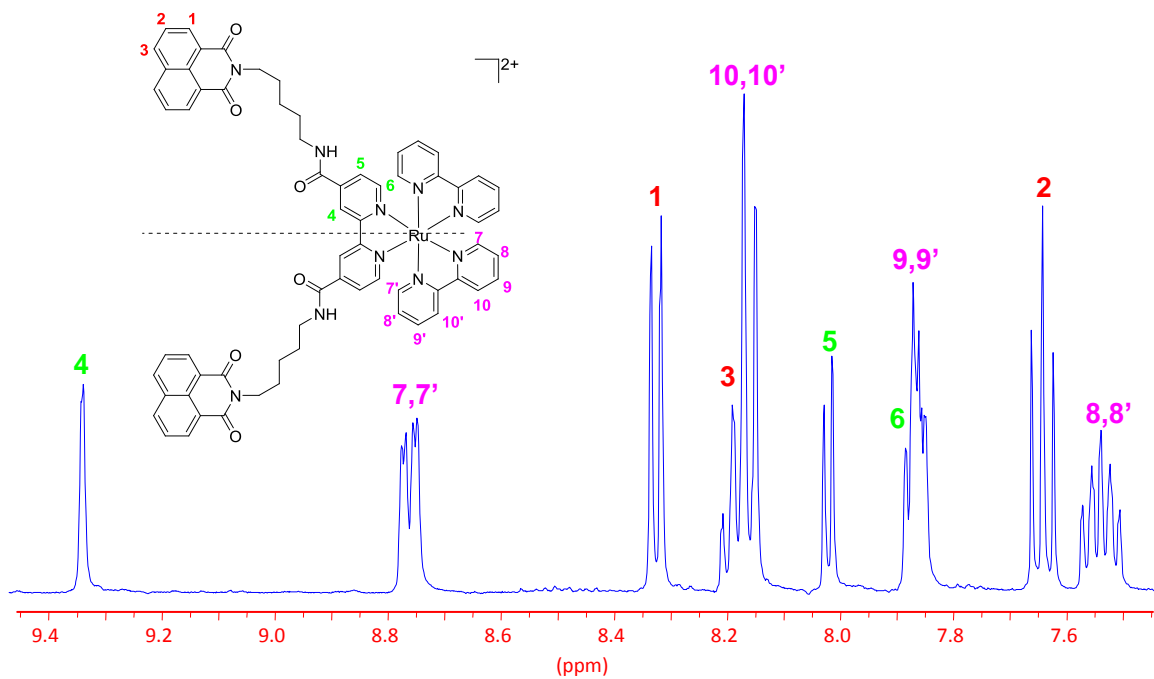


Figure S1 A) ¹H NMR (400 MHz, CD₃CN) of **Ru.Nap** and **B)** ¹H NMR (400 MHz, CD₃OD) of **Ru.2Nap** showing the aromatic regions.

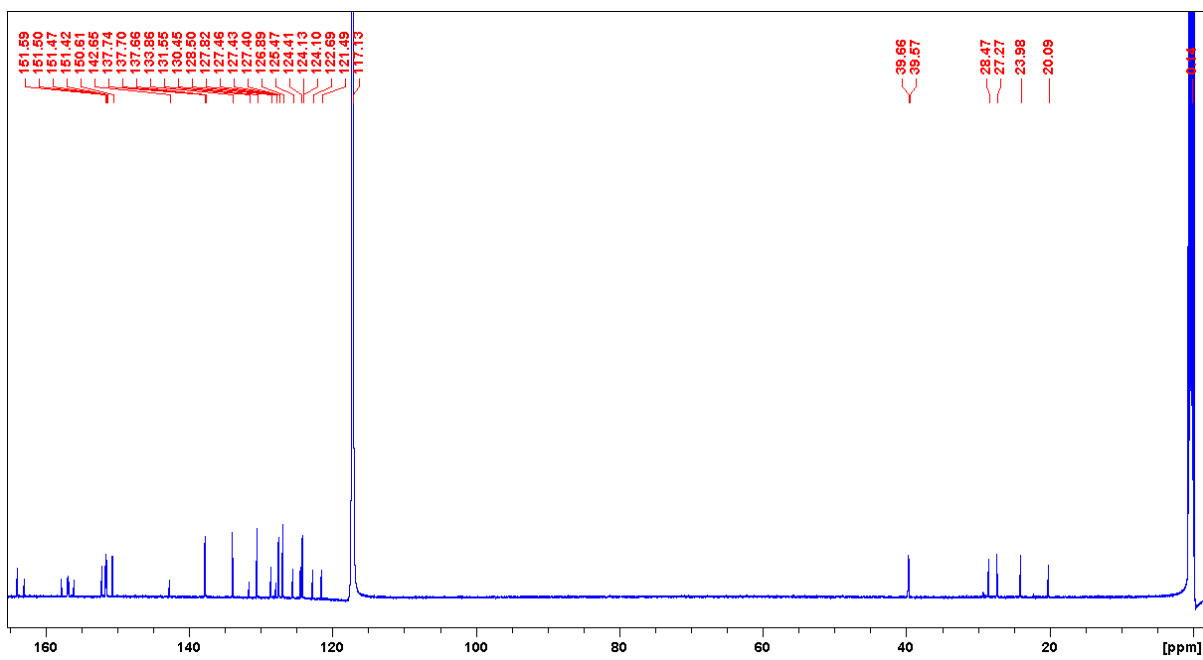


Figure S2 ¹³C NMR (150 MHz, CD₃CN) of Ru.Nap.

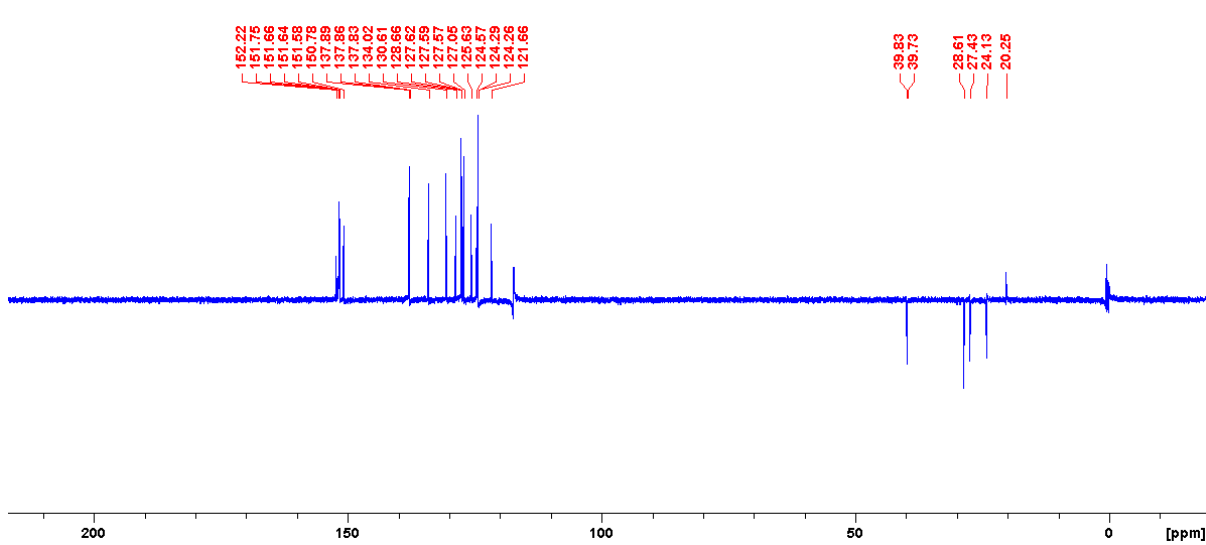


Figure S3 DEPT 135 NMR (150 MHz, CD₃CN) of Ru.Nap.

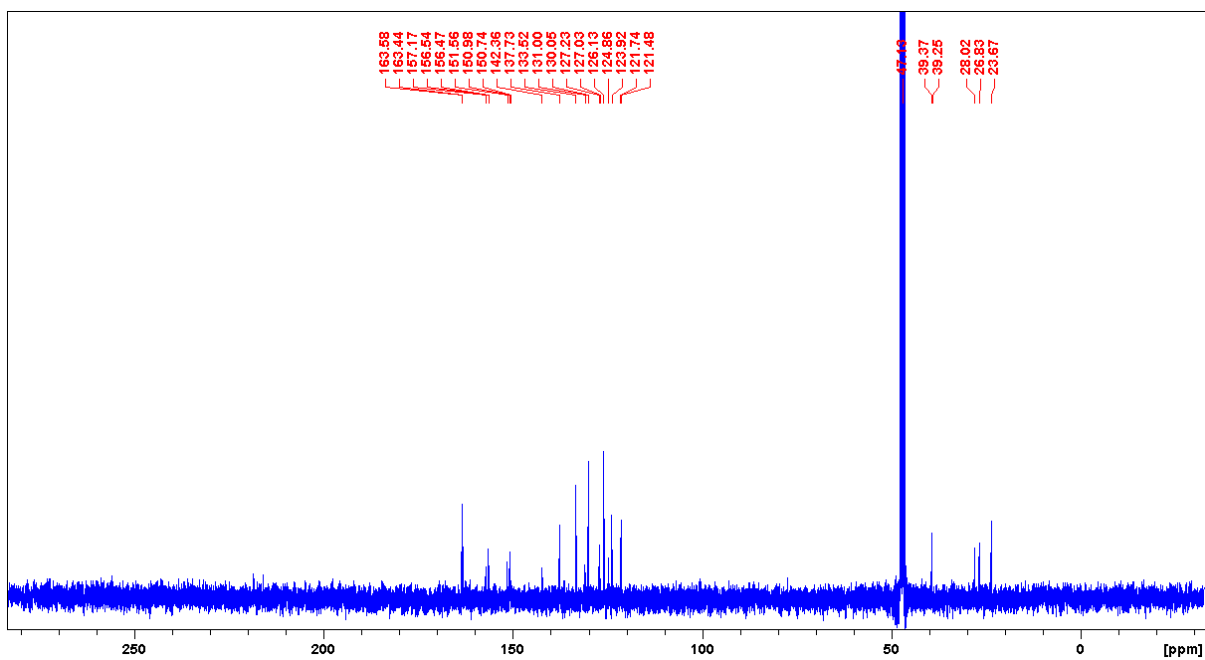


Figure S4 ¹³C NMR (100 MHz, CD₃OD) of Ru.2Nap.

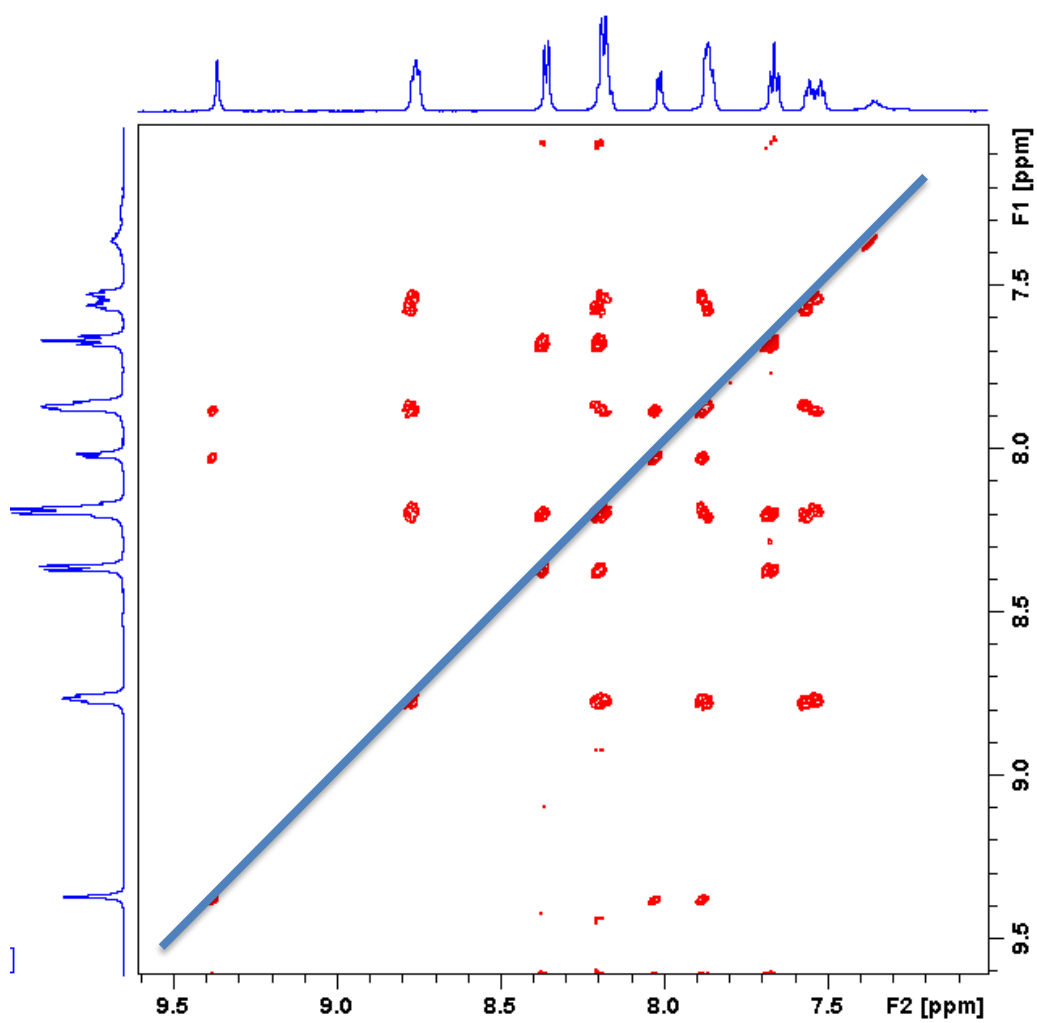


Figure S5 HH COSY spectrum (600 MHz, CD₃OD) of the aromatic region of **Ru.2Nap**.

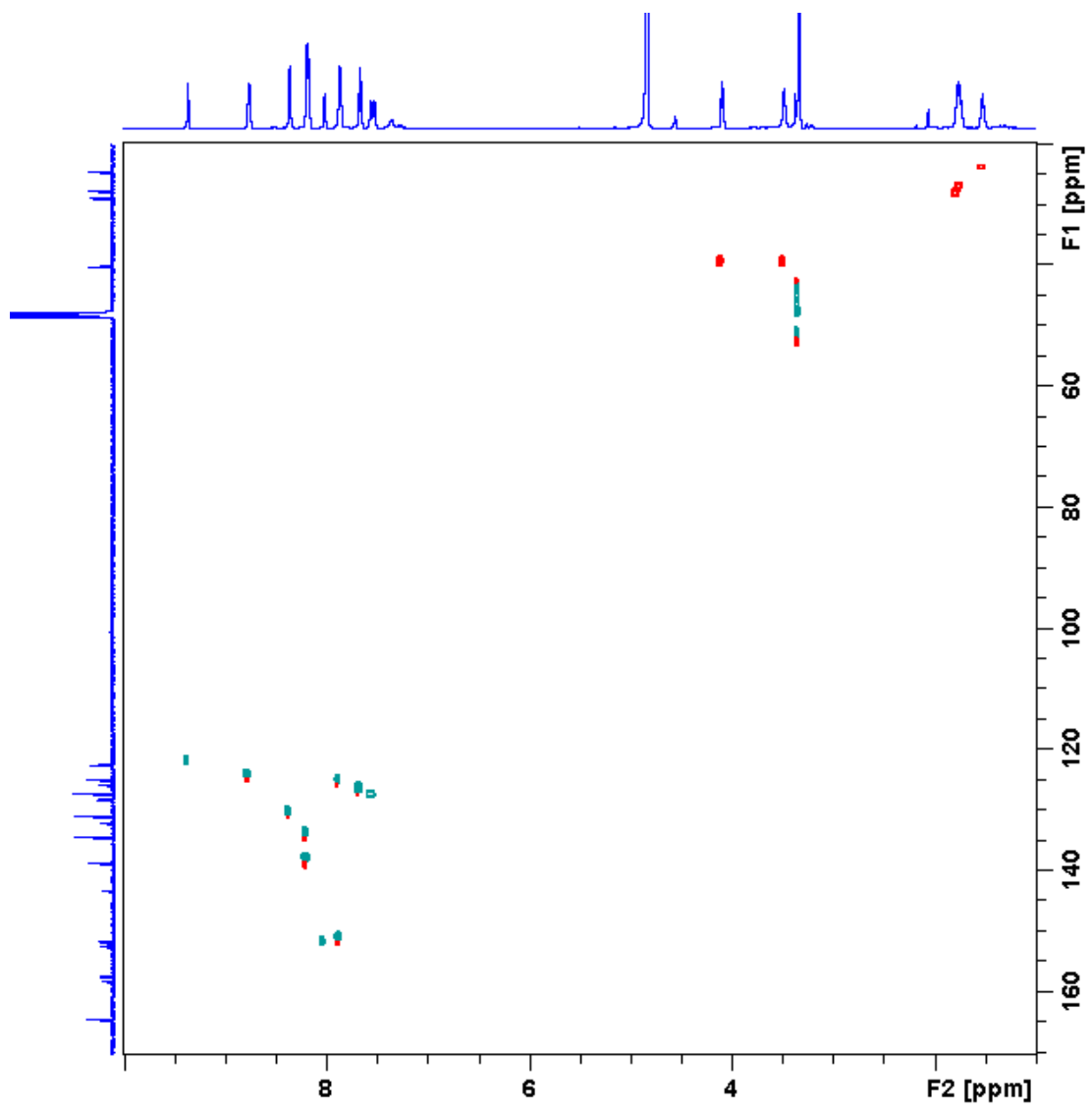


Figure S6 CH COSY spectrum (600 MHz, CD₃OD) of Ru.2Nap.

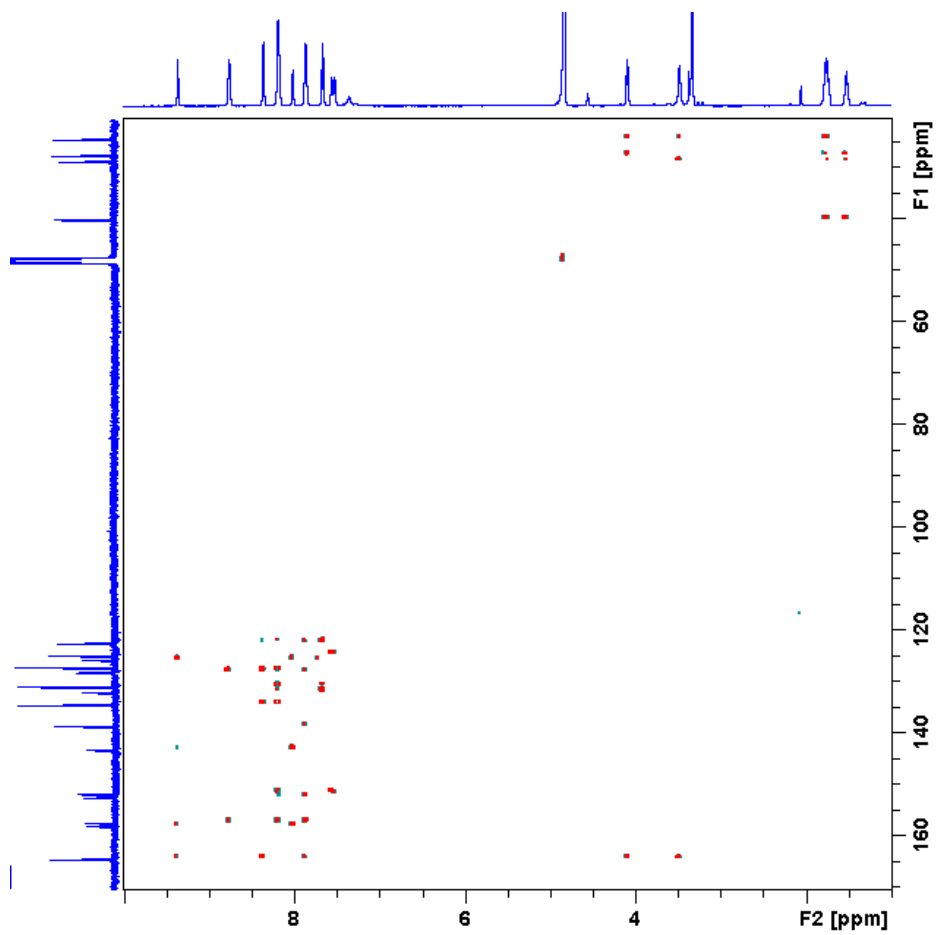


Figure S7 Long range CH COSY spectrum (600 MHz, CD₃OD) of **Ru.2Nap**.

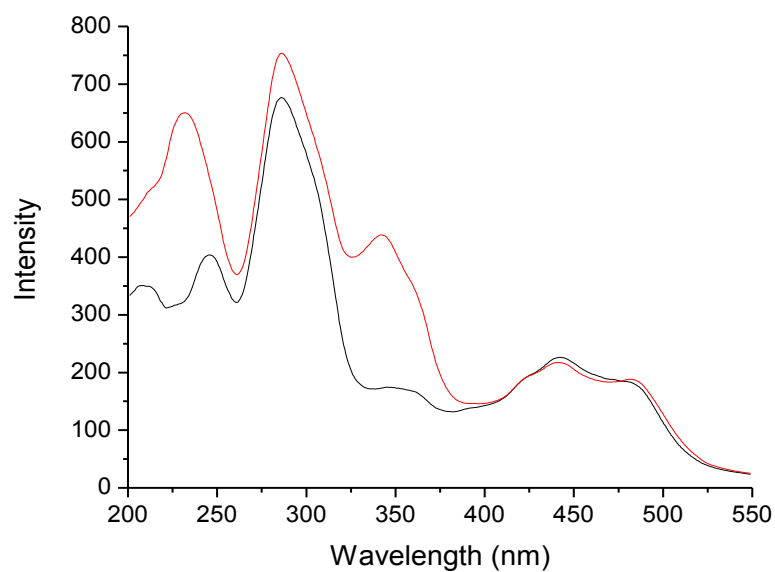


Figure S8 Excitation spectra (λ_{em} 670 nm) of **Ru** (—) and **Ru.2Nap** (—), both at 6.5 μ M in 10 mM phosphate buffer, at pH 7.

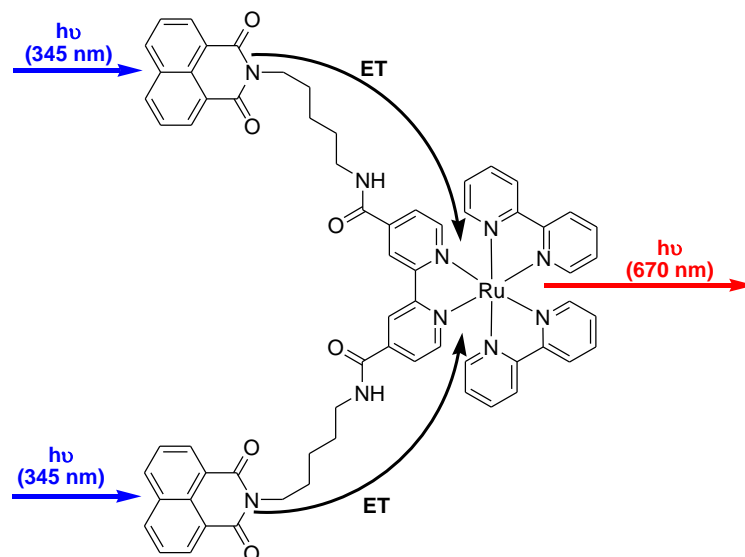


Figure S9 Representation of the antenna effect in which the excited state energy of the 1,8-naphthalimides is transferred to the Ru(II) MLCT excited state.

$$\Delta G = - [(E_{1/2} \text{Naph/Naph}^{\bullet -} - E_{1/2} \text{Ru}^{3+/2+})] - E^*$$

Equation S1 Simplified Rehm-Weller equation, from which a driving force for electron transfer for **Ru.Nap** and **Ru.2Nap** was determined. Where E^* is the excitation energy of the vibrationally relaxed MLCT excited state, estimated from the luminescence maximum.

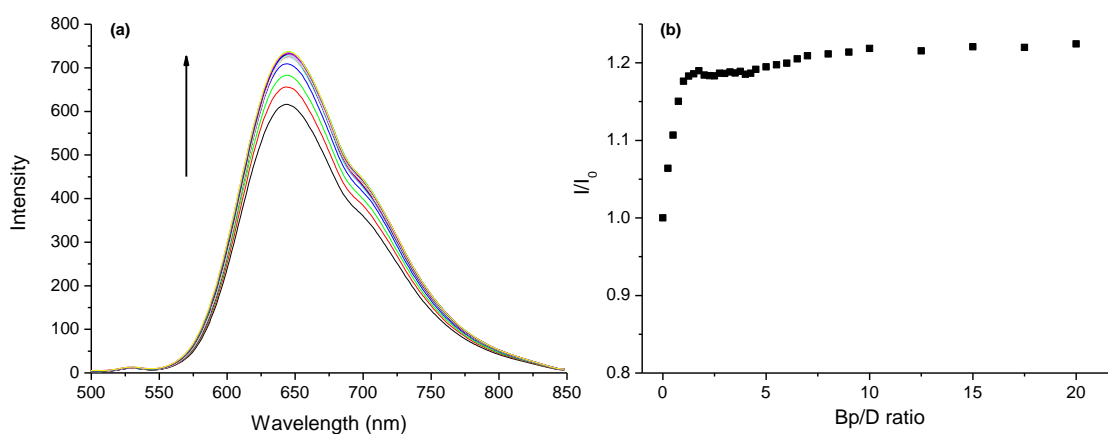


Figure S10 (a) Changes in the MLCT emission spectrum of **Ru.Nap** (6.5 μM) (λ_{ex} 450 nm) upon addition of st-DNA (0 – 130 μM base pairs) in 10 mM phosphate buffer, at pH 7. (b) The change in integrated MLCT emission intensity as a function of Bp/D.

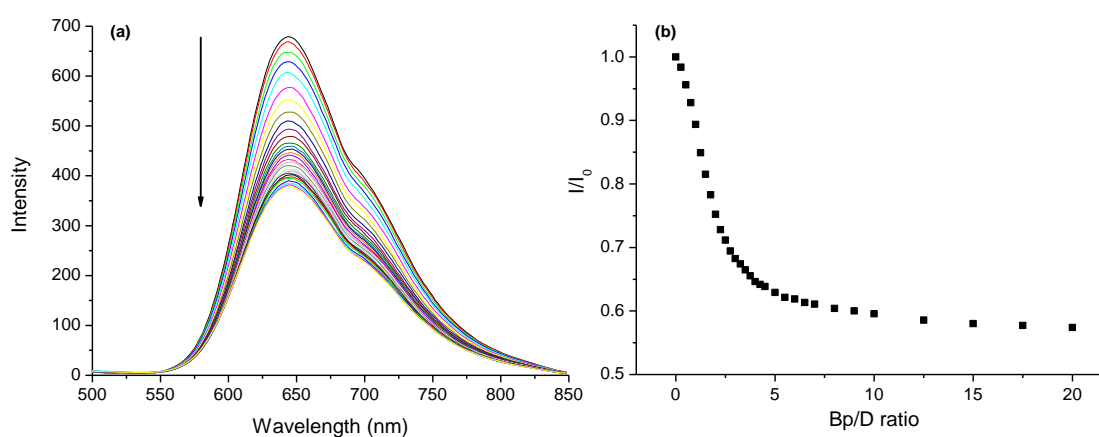


Figure S11 (a) Changes in the MLCT emission spectrum of **Ru.Nap** (6.5 μM) (λ_{ex} 338 nm) upon addition of st-DNA (0 – 130 μM base pairs) in 10 mM phosphate buffer, at pH 7. (b) The change in integrated MLCT emission intensity as a function of Bp/D.

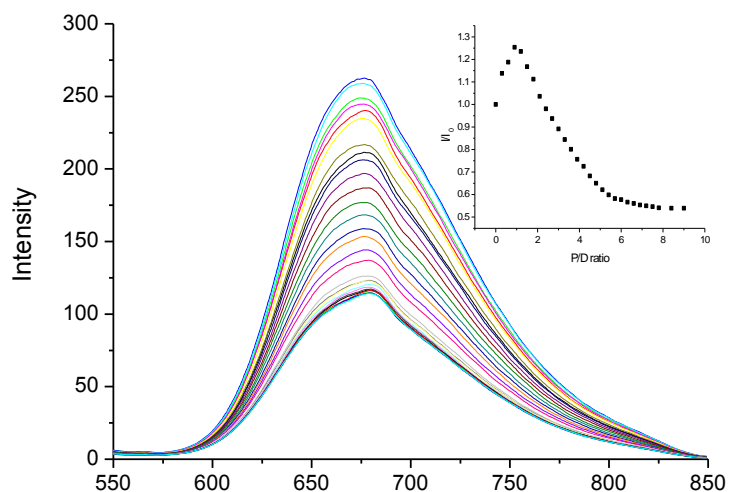


Figure S12 Changes in the MLCT emission spectrum of **Ru.2Nap** (6.5 μM) (λ_{ex} 450 nm) upon addition of st-DNA (0 – 29.25 μM base pairs) in 10 mM phosphate buffer, at pH 7. Inset: The change in integrated MLCT emission intensity as a function of Bp/D.

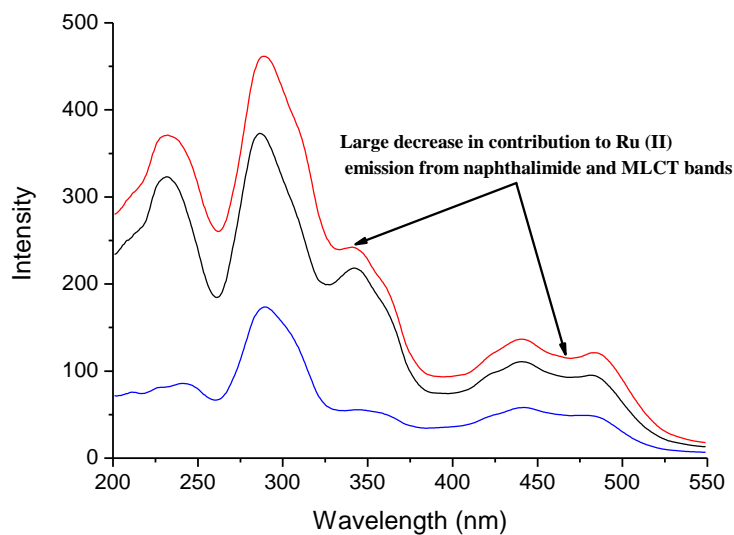


Figure S13 Excitation spectrum of **Ru.2Nap** (6.5 μM) (λ_{em} 670 nm) in 10 mM phosphate buffer, at pH 7 in the absence (—) and presence of st-DNA at a Bp/D ratio of 0.6 (—) and 4.5 (—).

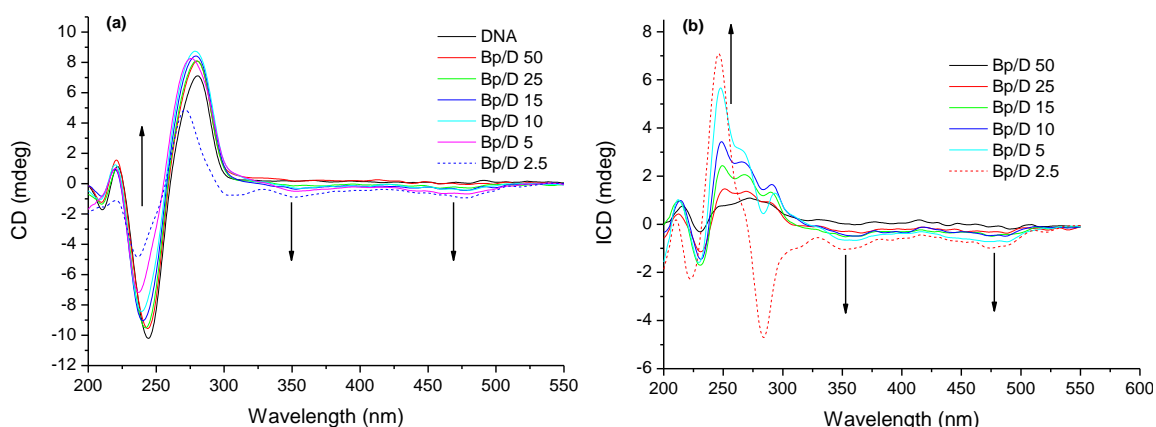


Figure S14 Circular dichroism curves of (a) st-DNA (150 μM) in 10 mM phosphate buffer, at pH 7 in the absence and presence of **Ru.2Nap** at varying ratios, and (b) the difference spectra obtained.

Lane	% Form I	% Form II
1	73	27
2	57	43
3	65	35
4	52	48
5	39	61
6	60	40
7	66	34
8	65	35

Table S1 Percentage of Form I vs II pBR322 plasmid DNA from the cleavage study in Fig. 11. Lane 1: Plasmid DNA control; Lane 2: $\text{Ru}(\text{bpy})_3^{2+}$ (Bp/D 5) 5 min irradiation; Lanes 3-5: **Ru.Nap** (Bp/D 5) 1, 3, 5 min respectively; Lanes 6-8: **Ru.2Nap** (Bp/D 5) 1, 3, 5 min respectively. Determination of the relative intensity of the bands showed that DNA was somewhat damaged to begin with, being comprised of 73% **Form I** and 27% **Form II**.

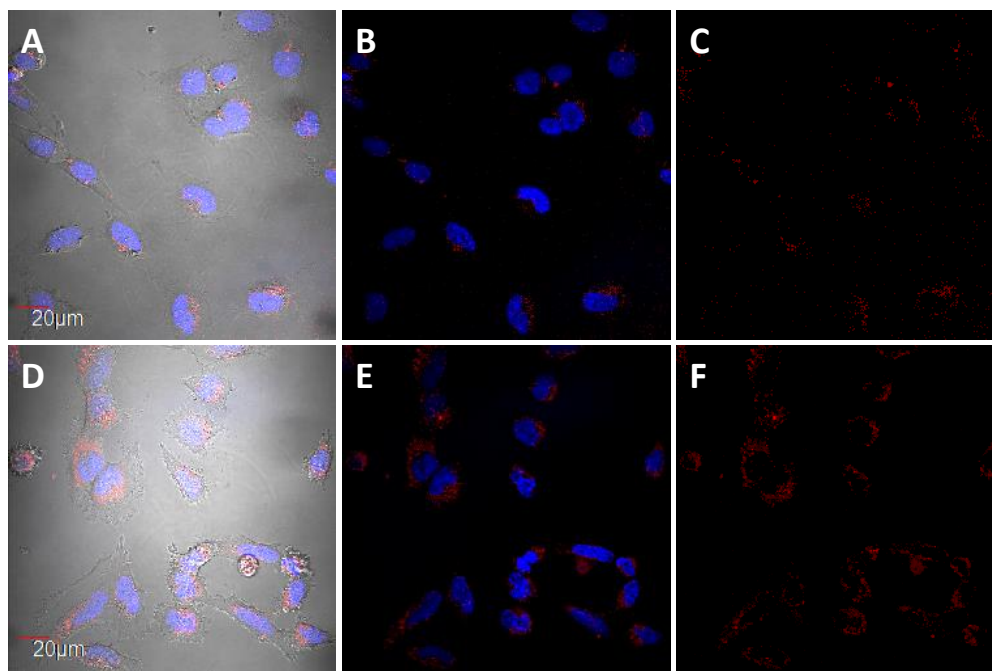


Figure S15 Confocal Laser Scanning Microscopy live cell images of **Ru.2Nap** (30 μ M) with HeLa cells. Shown are the images obtained with (A) the bright field view of treated cells after 4 hrs incubation, stained with DAPI (blue) and **Ru.2Nap** (red), (B) overlay of **Ru.2Nap** (red) and nuclear co-stain DAPI (blue), (C) **Ru.2Nap** emission alone (red), (D) the bright field view of treated cells after 24 hrs incubation, stained with DAPI (blue) and **Ru.2Nap** (red), (E) overlay of **Ru.2Nap** (red) and nuclear co-stain DAPI (blue), (F) **Ru.2Nap** emission alone (red).